

이리듐 배위 메소젠성 폴리플루오렌의 합성과 편광 전기발광 특성

곽부요 · 김기은* · 유창재* · 김재훈*[#] · 정광운** · 최이준^{#,†}

금오공과대학교 고분자공학과, *한양대학교 전자공학과, **전북대학교 고분자나노공학과
(2023년 4월 8일 접수, 2023년 6월 2일 수정, 2023년 6월 11일 채택)

Synthesis and Polarized Electroluminescence of Mesogenic Polyfluorenes Coordinated with Iridium

Puyao Guo, Gi-Eun Kim*, Chang-Jae Yu*, Jae-Hoon Kim*[#], Kwang-Un Jeong**, and E-Joon Choi^{#,†}

Department of Polymer Science and Engineering, Kumoh National Institute of Technology, Gumi, Gyeongbuk 39177, Korea

*Department of Electronic Engineering, Hanyang University, Seoul 04763, Korea

**Department of Polymer-Nano Science and Engineering, Jeonbuk National University, Jeonju 54896, Korea

(Received April 8, 2023; Revised June 2, 2023; Accepted June 11, 2023)

초록: 인광성 메소제닉 공중합체의 이색성을 평가하기 위하여 이리듐이 배워된 치환체를 곁사슬에 갖는 폴리플루오렌 공중합체를 합성하였다. 이때 벤조치아디아졸, 디옥틸플루오렌 및 이리듐착물-치환 플루오렌의 조성비를 1, 2, 5, 8, 11, 25 및 37.5 mol%로 변화시켰다. 합성한 공중합체의 구조 및 조성을 Fourier-transform infrared (FTIR) 및 proton nuclear magnetic resonance (¹H NMR) 분광분석법으로 조사하였다. 또한 공중합체의 UV-Vis 흡수, 광발광 및 전기발광 특성을 조사하였다. 공중합체의 분자량은 GPC 측정에 의해 7 내지 73 kDa 범위로 결정되었다. 결과적으로 배워된 이리듐착물-치환 플루오렌 구조를 1 mol% 및 5 mol%로 갖는 공중합체를 각각 적용한 전기발광 소자가 각각 가장 높은 휘도 및 가장 뚜렷한 이색성비(1.47)를 나타내었다.

Abstract: A series of phosphorescent mesogenic copolymers with various feed ratios of iridium-coordinating monomer as a side group have been prepared. Structure and composition of copolymers were confirmed by Fourier-transform infrared (FTIR) and proton nuclear magnetic resonance (¹H NMR) spectroscopy. Molecular weight of copolymers was determined to be in the range of 7 to 73 kDa by GPC measurement. UV-Vis absorption and photo- and electroluminescence properties of copolymers were investigated. As a result, copolymer IrCP-1 containing 1 mol% iridium-coordinating comonomer showed the highest luminance and current density. Copolymer IrCP-3 with 5 mol% iridium-coordinating comonomer exhibited a satisfactory dichroic ratio of 1.47.

Keywords: liquid crystalline polymer, polarized light, fluorescence, phosphorescent, electroluminescence.

Introduction

Nowadays, saving energy has always been the top issue in the world. Specifically, improving energy efficiency in the lighting technology can play an important role in energy conservation. As one of the most promising light sources, the organic light emitting diode (OLED) is attracting attention due to superior properties such as ultra-thin, transparent and flexible structure as well as low power consumption and excellent visual performance.^{1,2} Meanwhile, the emission efficiency

could be enhanced if luminescent materials were able to align itself to an ordered structure, which means the polarized light output could be realized.³⁻⁶ Over the last two decades, numerous studies have been made on polarized electroluminescence (EL) based on liquid crystalline (LC) materials to improve display efficiency.⁶⁻¹⁴ From a structural point of view, the mesogenic poly(fluorene)s including oligo(fluorene)s analogues have been considered as one of the prospective candidates for practical luminescent materials because of high luminescence as well as excellent mesogenic properties with good solubility in common solvents.¹²⁻¹⁴ It has been reported that the thermal and luminescent properties of mesogenic oligo(fluorene)s analogues are affected by the side chain length, and that the emission dichroism increases with the aspect ratio.^{11,12} Previous

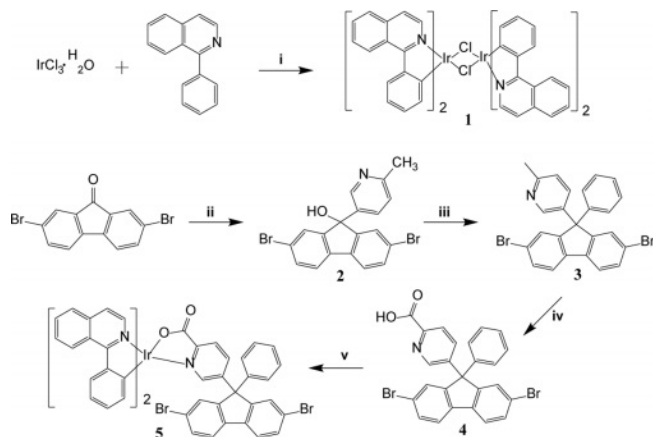
[#]These authors equally contributed to this work.

[†]To whom correspondence should be addressed.

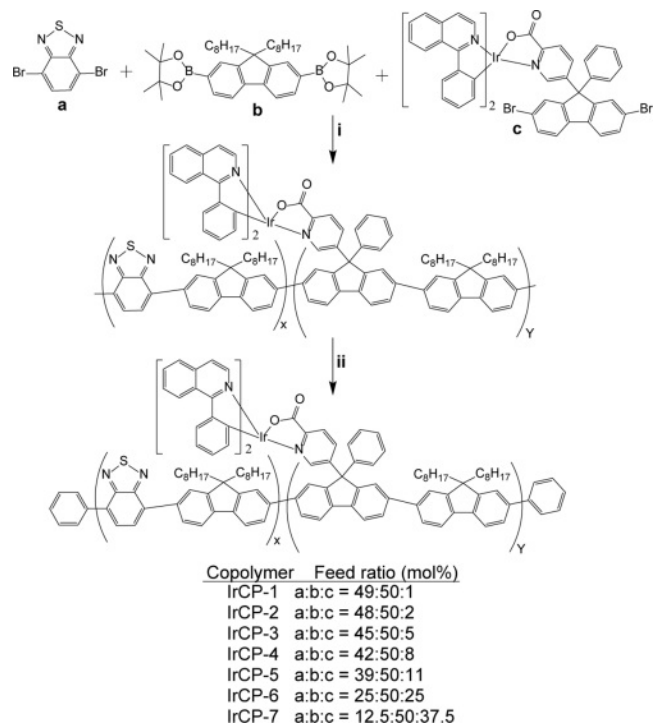
ejchoi@kumoh.ac.kr, ORCID[®] 0000-0002-6810-248X

©2023 The Polymer Society of Korea. All rights reserved.

work in Kim's group and others has shown that the polarization ratio for poly(9,9-di-n-octyl-fluorenyl-2,7-diyl)-alt-(benzo-[2,3,1]-thiadiazol-4,8-diyl) (F8BT) can be improved by the rubbing process using the commercial polyimide (PI) as an alignment agent.^{13,14} On the other hand, in the case of the non-polarized



Scheme 1. Synthetic route to the iridium-monomer; reagents and conditions: (i) 2-ethoxyethanol:H₂O = 3:1, reflux, 24 h; (ii) 5-bromo-2-methylpyridine, n-BuLi, ether, -78 °C to r.t., overnight, N₂ atmosphere; (iii) CF₃SO₃H, benzene, reflux, 6 h; N₂ atmosphere; (iv) KMnO₄, pyridine:H₂O = 3:1, reflux, 4 days; (v) Na₂CO₃, 2-ethoxyethanol, 100 °C, 24 h, N₂ atmosphere.



Scheme 2. Synthetic route to copolymers: reagents and conditions: (i) Pd(pph₃)₄, aq. K₂CO₃, toluene, Aliquat 336, 85 °C to 90 °C, 72 h; (ii) bromobenzene, reflux, 12 h; phenylboronic acid, reflux, 12 h.

emission of poly(fluorene)s, it has been attempted to control the luminescent colour and efficiency by means of copolymerization with a benzothiadiazole-based comonomer.¹⁵ To our knowledge, no studies have ever tried to examine the polarized luminescence for mesogenic fluorene copolymers of benzothiadiazole-based comonomer.

In general, high-efficiency OLEDs can be implemented with phosphorescent materials.¹⁶ A few phosphorescent LC polymers based on heavy metals have been reported.^{17,18} In particular, iridium complexes are most attractive because they have short triplet lifetimes and their emission can be tailored to cover visible wavelengths by changing the ligand.¹⁹ The most convenient way to achieve high-efficiency devices is to adopt blending the host fluorescent polymer with specific phosphorescent low MW dopants.²⁰⁻²³ However, this method often causes serious problems in phase separation that may lead to deficiency in thermal stability and defects in large-area fabrication. The most effective way to approach this issue is to introduce a phosphorescent chromophore directly into the polymer backbone.²⁴

In this study, new phosphorescent polarized light emissive polymers based on iridium complex were synthesized and characterized. Scheme 1 displays the synthetic route to iridium-coordinating monomer that the present authors abbreviated as the iridium-monomer for convenience. Scheme 2 presents the structure of copolymers synthesized by the Suzuki coupling reaction with varying the feed ratio of iridium-monomer. Diocetylfluorene unit was introduced to copolymers to ensure dichroic property and promote solubility and hence processibility. Benzothiadiazole group was introduced to impart copolymers with better charge-carrier mobility and the low bandgap.

Experimental

Materials and Instruments. Most chemicals were purchased from TCI (Japan) and Sigma Aldrich (USA), and used without further purification. Solvents were received from Daejung (Korea) and dried over 4 Å molecular sieves overnight before use. The silica gel 60 (a particle size of 0.040-0.063 mm) for column chromatography was purchased from Merck Co. (Germany). Analytical thin-layer-chromatography was performed using Aldrich silica gel thin layer chromatography (TLC) plates. The proton nuclear magnetic resonance (¹H NMR) and Fourier-transform infrared (FTIR) spectra were recorded on a Bruker Biospine 400 MHz NMR (USA) and a Thermo Fisher Scientific

Nicolet 6700 FTIR spectrometer (USA), respectively. The UV-Vis and photo-luminescence (PL) spectra were recorded on an Apex Scientific Optizen 3220UV (Ireland) and a Shimadzu RF-5401PC (Japan) spectrometer, respectively. The molecular weight of copolymers was determined by gel permeation chromatography (Shimadzu GPC, Japan). Thermal properties were investigated by differential scanning calorimetry (Netzsch DSC 200 F3, Germany) and thermo-gravimetric analysis (Irvine Materials Research Institute Auto-TGA Q500, USA). X-ray studies were conducted in the reflection mode using a Rigaku (Japan) 12 kW rotating anode X-ray (Cu K α radiation) generator coupled to a diffractometer. Cyclic voltammetry measurements were performed on a WizEcm-1200 Premium (USA): 0.1 M tetrabutylammonium perchlorate (TBAPC) and 0.1 M tetrabutylammonium hexafluorophosphate (TBAPF₆) were utilized as supporting electrolyte in CHCl₃ and tetrahydrofuran (THF) solution, respectively. The oxidation and reduction potentials were measured against an Ag/Ag⁺ reference electrode with a scan rate of 50 mV/s. The current density, voltage, and luminance characteristics of the OLED devices were evaluated using source meter (Keithley 2400, Keithley Instruments Inc., USA) and luminance meter (CS-1000, Konica Minolta, Japan). The spectra of polarized light were measured using an OceanOptics USB-2000 spectrometer (USA).

Synthesis of Monomer b. To a solution of 2,7-dibromo-9,9-dioctyl-9H-fluorene (5.00 g, 9.11 mmol) in THF (30 mL) was added n-BuLi (15.0 mL, 23.7 mmol) dropwise at -78 °C under a N₂ atmosphere. Then to the mixture was added 2-isopropoxy-4,4,5,5-tetramethyl-1,3,2-dioxaborolane (5.60 mL, 27.4 mmol). The resulting mixture was stirred at -78 °C for 1 h, warmed to 0 °C, and stirred for another 12 h at room temperature. The reaction mixture was poured into water and extracted with ethyl ether. The crude product was purified by flash chromatography on silica gel with a mixture of hexane and dichloromethane (DCM) as eluent. Recrystallization from ethanol afforded pure product. Yield 57%. IR (KBr) cm⁻¹: 2990 (ArCH), 2930 (CH), 1344 (ArC=C), 1136 (BC). ¹H NMR (CDCl₃) δ : 0.78 (t, 6H, *J* = 7.1 Hz), 1.2 (m, 24H), 1.37 (s, 24H), 2.0 (m, 4H), 7.71 (t, 4H, *J* = 13.5 Hz), 7.78 (d, 2H, *J* = 7.9 Hz).

Synthesis of Compound 1. To a solution of iridium (III) chloride hydrate (1.00 g, 3.35 mmol) in a mixture of 2-ethoxyethanol and water (v/v = 3:1) (150 mL) was added 1-phenylisoquinoline (1.72 g, 8.37 mmol). The mixture was refluxed for 24 h. After reaction, water was added, and the resulting precipitate was filtered and washed with ethanol and diethyl ether

to afford the product as a red powder. Yield 78%. IR (KBr) cm⁻¹: 3011 (ArCH), 1640 (CN), 1408 (CH). ¹H NMR (CDCl₃) δ : 6.01 (d, 4H, *J* = 7.8 Hz), 6.48 (t, 4H, *J* = 8.1 Hz), 6.53 (d, 4H, *J* = 6.3 Hz), 6.79 (t, 4H, *J* = 8.2 Hz), 7.73 (m, 4H), 7.83 (m, 8H), 8.10 (d, 4H, *J* = 7.8 Hz), 8.95 (d, 4H, *J* = 8.5 Hz), 9.02 (d, 4H, *J* = 6.4 Hz).

Synthesis of Compound 2. Under a nitrogen atmosphere at -78 °C over 30 min, n-BuLi (12.0 mL, 19.2 mmol) was added dropwise into a solution of 5-bromo-2-methylpyridine (3.00 g, 17.4 mmol) in dry ether (30 mL). The reaction mixture was stirred at -78 °C for 10 minutes. It was then warmed to 0 °C and stirred for 1 hour. Then cool again to -78 °C. After that, 2,7-dibromo-9-fluorenone (5.89 g, 17.4 mmol) was added in three portions. The reaction mixture was warm to room temperature and stirred overnight. After reaction, mixture was poured into water and extracted using ethyl acetate. The organic layer was washed thoroughly with water and dried over magnesium sulphate. After the rotary-evaporation, the obtained residue was purified by flash column chromatography on silica gel with a mixture of DCM and ethyl acetate as eluent to afford product. Yield 81%. IR (KBr) cm⁻¹: 3083 (OH), 2800 (CH), 1454 (ArC=C), 1406 (CN), 1249, 1157 (CO). ¹H NMR (acetone-d₆) δ : 2.43 (s, 3H), 5.75 (s, 1H), 7.15 (d, 1H, *J* = 8.1 Hz), 7.46 (d, 2H, *J* = 2.0 Hz), 7.55 (dd, 1H, *J* = 8.1, 2.4 Hz), 7.60 (dd, 2H, *J* = 10.0, 6.2 Hz), 7.80 (d, 2H, *J* = 8.1 Hz), 8.41 (d, 1H, *J* = 2.0 Hz).

Synthesis of Compound 3. To a solution of compound 2 (2.80 g, 6.49 mmol) in dry benzene (100 mL) was added dropwise trifluoromethane-sulfonic acid (1.15 mL, 13.0 mmol) under nitrogen atmosphere. The solution was then refluxed for 6 h. After reaction, mixture was poured into sodium bicarbonate saturated solution and extracted with ethyl acetate. Organic layer was then washed by excessive water and dried over magnesium sulphate. After the rotary-evaporation, the obtained residue was purified by flash column chromatography with DCM as eluent on silica gel to afford product. Yield 82%. IR (KBr) cm⁻¹: 3032 (ArCH), 1608, 1492 (C=C), 1463 (CN), 750 (CBr). ¹H NMR (CDCl₃) δ : 2.45 (s, 3H), 7.17 (d, 1H, *J* = 9.1 Hz), 7.21 (d, 1H, *J* = 1.6 Hz), 7.23 (d, 1H, *J* = 1.9 Hz), 7.32 (m, 3H), 7.49 (dd, 1H, *J* = 8.1, 2.6 Hz), 7.64 (m, 4H), 7.92 (d, 2H, *J* = 8.1 Hz), 8.27 (d, 1H, *J* = 2.5 Hz).

Synthesis of Compound 4. To a refluxed solution of compound 3 (1.30 g, 2.65 mmol) in a mixture of H₂O and pyridine (1:3 v/v) (60 mL) was added KMnO₄ (6.27 g, 39.7 mmol) in ten portions over 4 days. After that, reaction mixture was filtered, and the obtained filtrate was acidified with conc. HCl to

pH 3.0. The resulting precipitate was washed with water and methanol. The crude product was purified using a flash column chromatography with ethyl acetate as an eluent. The residue was washed with methanol and CHCl_3 to remove residual silica gel thoroughly. The removal of the solvent afforded product. Yield 20%. IR (KBr) cm^{-1} : 3393 (OH), 1627 (CO), 1547 (ArC=C), 1430 (CN), 1400 (CO). ^1H NMR (CDCl_3) δ : 7.21 (m, 2H), 7.30 (m, 3H), 7.45 (s, 2H), 7.52 (d, 2H, $J = 8.2$ Hz), 7.65 (d, 2H, $J = 8.5$ Hz), 7.77 (m, 1H), 8.01 (d, 2H, $J = 7.8$ Hz), 8.65 (s, 1H).

Synthesis of Compound 5. To 35 mL of 2-ethoxyethanol was added compound 1 (1.30 g, 1.10 mmol), compound 4 (1.44 g, 2.76 mmol) and Na_2CO_3 (1.17 g, 11.0 mmol). Under a nitrogen atmosphere, the mixture was stirred at 100 °C for 24 h. After reaction, mixture was filtered and the resulted precipitate was washed with hexane and ethanol thoroughly to afford product. Yield 78%. IR (KBr) cm^{-1} : 3051 (ArCH), 1647 (C=O), 1551(ArC=C), 1431 (CN), 1300 (CO). ^1H NMR (CDCl_3) δ : 6.20 (d, 1H, $J = 7.6$ Hz), 6.31 (d, 1H, $J = 8.5$ Hz), 6.54 (m, 1H), 6.63 (dd, 1H, $J = 8.5, 1.2$ Hz), 6.65 (d, 1H, $J = 1.9$ Hz), 6.70 (d, 2H, $J = 7.4$ Hz), 6.89 (t, 1H, $J = 8.2$ Hz), 6.97 (d, 1H, $J = 1.6$ Hz), 7.02 (t, 2H, $J = 7.8$ Hz), 7.17 (d, 1H, $J = 1.6$ Hz), 7.19 (d, 1H, $J = 5.2$ Hz), 7.24 (d, 2H, $J = 1.9$ Hz), 7.39 (m, 1H), 7.41 (d, 1H, $J = 1.7$ Hz), 7.48 (d, 1H, $J = 1.4$ Hz), 7.50 (d, 2H, $J = 5.8$ Hz), 7.52 (d, 1H, $J = 5.8$ Hz), 7.7 (m, 3H), 7.75 (m, 2H), 7.86 (m, 1H), 7.91 (d, H, $J = 8.3$ Hz), 7.94 (d, 1H, $J = 2.1$ Hz), 8.08 (d, 1H, $J = 8.2$ Hz), 8.15 (d, 1H, $J = 8.0$ Hz), 8.72 (d, 1H, $J = 6.4$ Hz), 8.85 (d, 1H, $J = 7.6$ Hz), 8.91 (m, 1H).

Copolymerization. To toluene was added a mixture of monomers a, b and c with an appropriate feed ratio shown in Scheme 2, which correspond to 4,7-dibromobenzo[c]-1,2,5-

thiadiazole, 2,2'-(9,9-di-octyl-9H-fluorene-2,7-diyl)-bis(4,4,5,5-tetramethyl-1,3,2-dioxaborolane), and compound 5 in this paper. To this solution were added aqueous potassium carbonate (2M) and Aliquat 336 (methyltriocetyl ammonium). Then this mixture was degassed, tetrakis(triphenylphosphine)palladium(0) was added, and stirred at 85-90 °C for 72 h. To terminate the polymerization, bromobenzene and phenylboronic acid were used to cap the chain end groups of the polymers by refluxing for 12 hours each. The resulting reaction mixture was poured into a mixture of methanol and water (2:1 v/v) and filtered. The resulting precipitate was washed with water, methanol, ethanol and acetone in this order. Reprecipitation using chloroform and methanol as a solvent/non-solvent pair afforded the desired polymer product.

Fabrication of OLED Device. Fabrication process of aligned emissive layer (EML) and structure of EL device are presented in Figure 1. Copolymers were dissolved in CHCl_3 for spin coating. Prepatterned ITO substrates with a sheet resistance of $\approx 20 \Omega/\text{sq}$ were rinsed in an ultrasonic bath for 60 min with deionized water and an alkali detergent (mucosol). Copper phthalocyanine (CuPC) with thickness of 2 nm was commercially acquired from Lumtec (Taiwan), and was deposited by thermal evaporation with high-vacuum (6×10^{-6} torr) on ITO, as a hole injection layer. A polyimide (PI) AL22636 (JSR, Japan) was used as an alignment layer for EML. The PI was spin-coated on the CuPC layer, and unidirectionally rubbed by a 6.5 cm diameter roller covered with cotton cloth. The dissolved copolymers in CHCl_3 were spin-coated at 3000 rpm for 20 s followed by at 1000 rpm for 10 s to obtain the 50 nm thickness layer on the rubbed PI. For EL devices, 1,3,5-tris(N-phenylbenzimidazol-2-yl)-benzene (TPBi, 20 nm), LiF (1 nm) and Al (70 nm) were deposited by thermal evaporation with high vacuum (6×10^{-6} torr) as an HBL to confine excitons in the EML, electron injection layer, and cathode, respectively. All EL samples were encapsulated by glass and an optical UV curable resin (NOA 65) to avoid exposure to atmospheric oxygen and humidity.

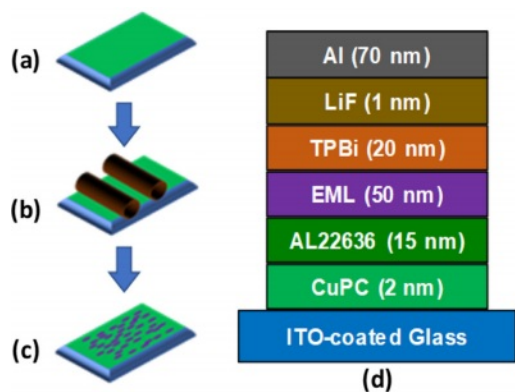


Figure 1. Fabrication of aligned emissive layer (EML): (a) spin coating of PI alignment layer on ITO surface; (b) rubbing process; (c) spin coating of copolymers and thermal annealing at 270 °C for 10 min; (d) multilayer structure of EL device.

Results and Discussion

Molecular Weight and Composition Information. In Table 1, the number average molecular weight (M_n) of the copolymers was determined by GPC to be in the range of 6600 to 73000 with a polydispersity index (PDI) of 1.62 to 3.33. It was found that the molecular weights tend to decrease with increasing iridium feed ratio, which implies that a higher amount of iridium

Table 1. Composition and MW information of copolymers

Copolymer code	Feed ratio ^a (mol%)	Composition ^b (mol%)	M_n (kDa)	M_w (kDa)	PDI
IrCP-1	1	- ^c	73	147	2.0
IrCP-2	2	- ^c	46	154	3.3
IrCP-3	5	6.7	26	52	2.0
IrCP-4	8	6.5	14	28	2.0
IrCP-5	11	10.2	17	37	2.2
IrCP-6	25	15.2	7	11	1.6
IrCP-7	37.5	33.3	- ^d	- ^d	- ^d

^aContent of iridium-monomer. ^bEstimated from ¹H NMR. ^cNMR-resonance for IrCP-1 and IrCP-2 was too weak to calculate composition. ^dCopolymer with 37.5 mol% feed ratio of iridium-monomer provided no GPC information due to its poor solubility in THF.

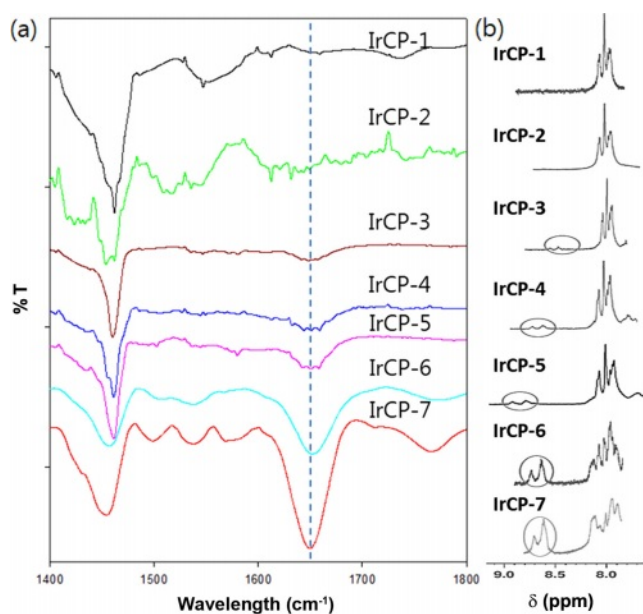


Figure 2. (a) Normalized FTIR spectra of copolymers (KBr pellet); (b) ¹H NMR spectra of copolymers (s = CDCl₃); the circles indicate NMR resonance for Ir(piq)₂.

monomer might lead less effective polymerization process. The structure of copolymers was investigated by FTIR and ¹H NMR spectroscopy, which contain an iridium(II) complex coordinated with bis(phenyl isoquinoline) and picolinato ligands, *i.e.* (piq)₂Ir(pic), as a pendant group. In Figure 2(a), the FTIR spectra of copolymers show the adsorption peaks for C=O stretching of the picolinato ligand at about 1650 cm⁻¹ and for aromatic C=C at about 1470 cm⁻¹. As the iridium-monomer content increased in the feed ratio, the intensity of the former peak became more prominent than that of the latter peak. As shown in Figure 2(b), the NMR resonance peaks caused by

Table 2. Thermal and Photophysical Properties of Copolymers

Code	T_g (°C)	T_d (°C)	UV λ_{max} (nm)	PL λ_{max} (nm)
IrCP-1	104	421	320, 336, 456	535, 650
IrCP-2	112	309	320, 335, 456	525, 644
IrCP-3	105	368	320, 336, 448	510, 643
IrCP-4	106	390	318, 337, 451	523, 643
IrCP-5	103	384	319, 337, 453	515, 640
IrCP-6	123	346	319, 333	512, 640
IrCP-7	150	290	373	513, 640

(piq)₂Ir(pic) were detected at $\delta = 6.3$ -7.0 ppm and at 8.7-9.0 ppm. The intensity of these peaks became stronger when the content of iridium-monomer increases in the feed ratio. By comparing the integral of the NMR peaks derived from the aromatic protons of (piq)₂Ir(pic) with those from the aliphatic protons of the fluorene side chain, the copolymer composition was determined, and the results are summarized in Table 1. There is a somewhat difference between the feed ratio and copolymer composition. For IrCP-1 and IrCP-2 copolymers, the NMR-resonance due to the presence of (piq)₂Ir(pic) was too weak to calculate the copolymer composition. The results suggested that the composition of obtained copolymers was somewhat different from the feed ratio of comonomers.

Thermal and X-ray Diffraction Properties. Thermal properties were investigated by DSC and TGA. Glass transition temperatures (T_g) were determined from the second DSC heating cycle. Thermal decomposition temperatures (T_d), defined as 5% weight loss under nitrogen atmosphere, were measured by TGA at a heating rate of 20 °C/min. The thermal data was summarized in Table 2. The T_g and T_d of copolymers were 103 °C to 150 °C and 290 °C to 421 °C, respectively. In general, it was found that with increasing iridium content the T_g values tend to increase while T_d values to decrease.

Figure 3(a) shows the XRD patterns of copolymers measured at ambient temperature. All copolymers showed broad diffraction patterns in the wide-angle region. Except for IrCp-4 and IrCP-5 copolymers, the rest of copolymers showed a strong reflection peak at small-angle region. The results suggest that the crystallinity of IrCp-4 and IrCP-5 might be sufficiently low to be considered amorphous. The temperature dependence of the diffraction for IRCP-3, which showed the strongest reflection intensity on the low angle side, was investigated. Figure 3(b) displays there was no significant change in the diffraction pattern with increasing temperature. Note that the expected crystalline pattern caused by the (piq)₂Ir(pic) com-

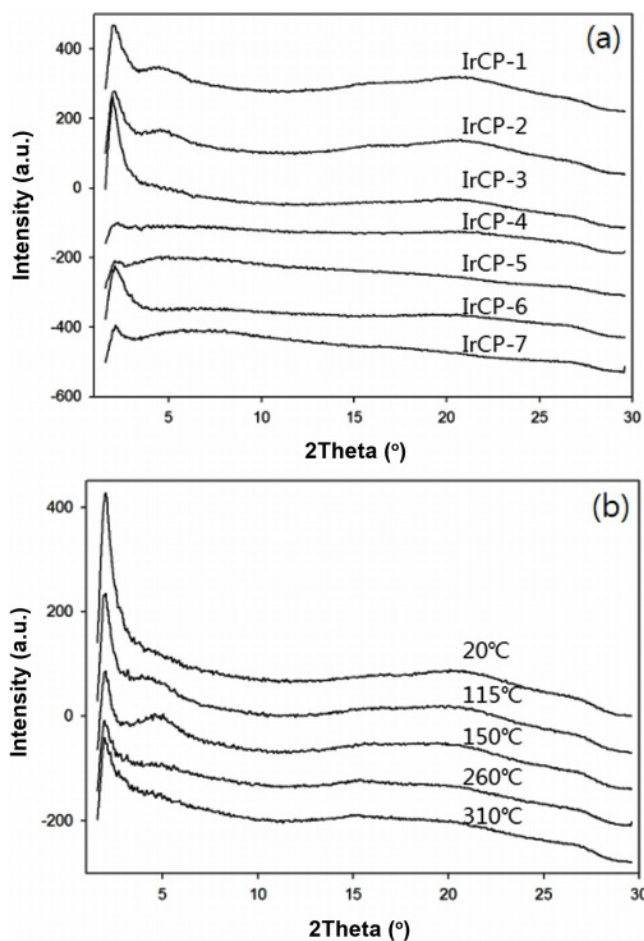


Figure 3. (a) X-ray diffraction (XRD) patterns of copolymers; (b) XRD patterns for IrCP-3 measured at given temperature.

plex structure was not detected in the wide-angle region. We have postulated that the copolymers do not have regular chain packing and would have regularity according to their repeated structural units.

Photophysical and Electrochemical Properties. UV-Vis absorption and PL data of copolymers were measured in dilute chloroform solution and excitation wavelength for PL measurements was 319 nm. The resulting spectra are shown in Figure 4 and summarized in Table 2. It is obvious that copolymers IrCP-1 to IrCP-5 showed similar absorptions around 320 nm, 336 nm and 456 nm. When the content of iridium-monomer increases, the absorptions around 320 nm and 336 nm become progressively stronger compared to those at 456 nm. As in IrCP-6, a further augmentation of iridium load caused broadening the absorption peak and minor shifting to 319 nm and 333 nm with trace absorption of 450 nm. Finally, IrCP-7 exhibited the strongest single absorption peak at 373 nm due to iridium complex moiety.

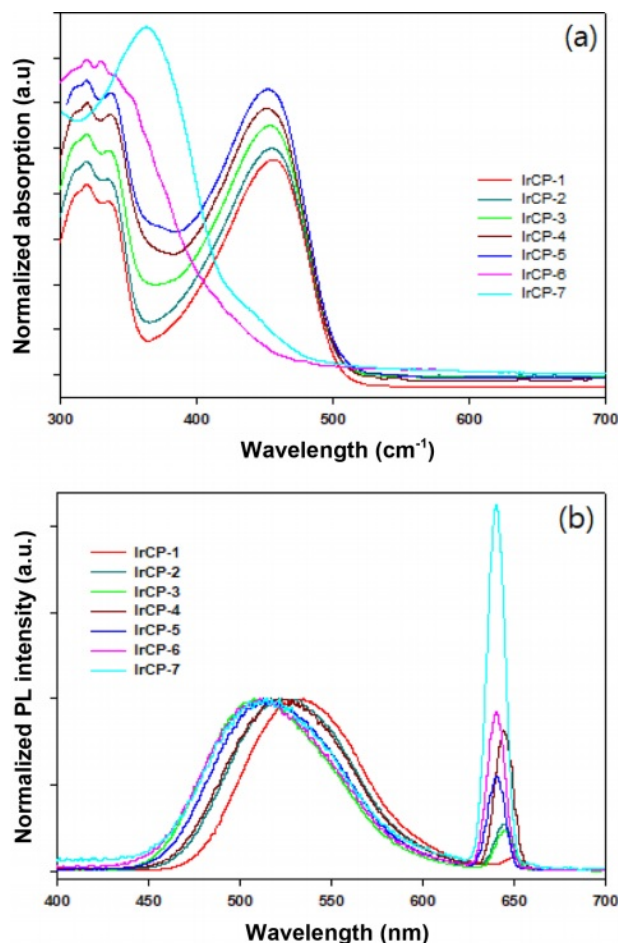


Figure 4. (a) UV-Vis absorption spectra of copolymers in dilute CHCl₃ solution with various feed ratios of iridium-monomer; (b) PL spectra of copolymers in dilute CHCl₃ solution with excitation wavelength of 319 nm.

This implies that the effect of introduction of iridium appears gradually until the composition of iridium-monomer is about 10 mol%, but it becomes predominant at about 30 mol% through 15 mol% intermediate steps.

PL spectra are presented in Figure 4(b). All copolymers showed two PL emissions at about 520 nm and 640 nm. As the content of iridium-monomer increased in copolymer composition, the PL emissions of 535 nm were blue-shifted without any relative intensity change, whereas those of 650 nm were blue-shifted with a gradual increase in intensity. Interestingly, UV-vis absorption spectra partially overlap with emission spectra. This indicates that the efficient energy transfer might be possible in this system.

Cyclic voltammetry measurements were performed to study the electrochemical properties of copolymers. Ferrocene was used as internal standard. The onset oxidation potential of

Table 3. Energy Levels of Copolymers^a

Code	E_{ox} (V)	HOMO (eV)	E_{red} (V)	LUMO (eV)	E_{g} (eV)	E_{g}^b (eV)
IrCP-1	1.74	-5.97	-0.52	-3.38	2.59	2.47
IrCP-2	1.63	-5.86	-0.82	-3.41	2.45	2.48
IrCP-3	1.66	-5.89	-0.78	-3.45	2.44	2.48
IrCP-4	1.67	-5.90	-0.86	-3.37	2.53	2.48
IrCP-5	1.64	-5.87	-0.78	-3.45	2.42	2.48
IrCP-6	1.56	-5.79	-0.81	-3.42	2.37	2.48
IrCP-7	0.56	-4.87	-1.24	-3.07	1.80	2.51

^aHOMO and LUMO energies were calculated from the empirical equations: $E_{\text{HOMO}} = -4.8 - [E_{\text{ox(onset)}} - E_{\text{ox(ferrocene)}}]$ eV; $E_{\text{LUMO}} = -4.8 - [E_{\text{red(onset)}} - E_{\text{ox(ferrocene)}}]$ eV. ^bOptical bandgap of each copolymer was calculated from the equation: $E = 1240/\lambda_{\text{onset}}$.

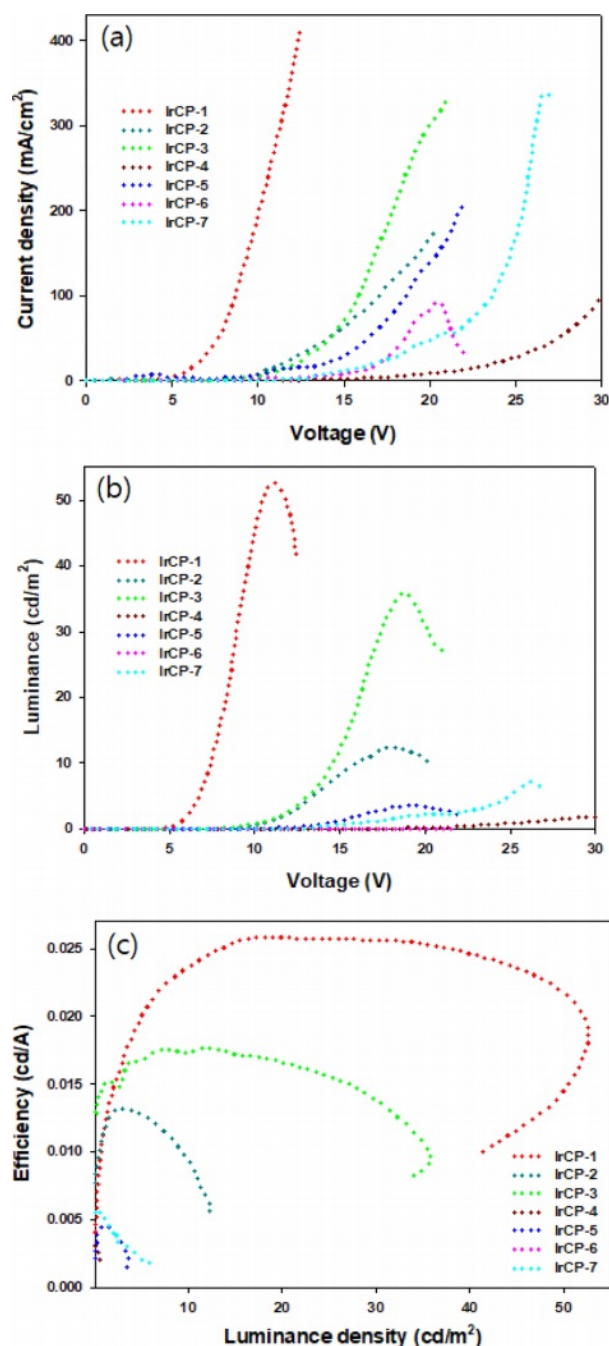
Table 4. EL and Dichroic Properties Copolymers

Code	EL λ_{max} (nm)	Turn-on voltage ^a (V)	J^b (mA/cm ²)	L_{max}^c (cd/m ²)	η^d (cd/A)	Dichroic ratio
IrCP-1	540	5.5	416	52.7	0.0257	1.00
IrCP-2	543	6.5	182	12.3	0.0132	0.99
IrCP-3	543	7.5	331	35.6	0.0188	1.47
IrCP-4	543, 614	12	98	- ^e	- ^e	0.98
IrCP-5	543, 623	2.5	213	3.6	0.0045	1.00
IrCP-6	543, 656	8.5	335	7.1	- ^e	1.00
IrCP-7	656	10	94	- ^e	0.0072	1.01

^aVoltage was measured at 1 cd/m². ^bMaximum current intensity. ^cMaximum luminance. ^dMaximum efficiency. ^eNot available.

ferrocene, $E_{\text{ox(ferrocene)}}$ in THF and chloroform were measured as 0.57 V and 0.49 V, respectively. The HOMO and LUMO energy levels were calculated according to the empirical formula as shown in Table 3. As a result of CV measurements, it was found that bandgaps of copolymers seem to get narrower with increasing iridium load.

Electroluminescent and Dichroic Properties. In order to study the EL properties of copolymers, EL devices based on copolymers have been made (see Figure 1). Figures 5 and 6 show the EL characteristics of devices based on copolymers, and related information was summarized in Table 4. Figure 5(a) shows the current density-voltage characteristics of devices. The turn-on voltages of copolymers ranged from 2.5 V to 12 V regardless of feed ratio. The device based on IrCP-1 exhibited the highest current density of 416 mA/cm² at 12.5 V. Figure 5(b) shows the luminance-voltage characteristics of devices. In

**Figure 5.** Plots of (a) current density vs. voltage; (b) luminance vs. voltage; (c) current efficiency vs. luminance density.

general, the maximum luminance (L_{max}) tended to increase as the content of iridium-monomer decreased, and ranged from 3.6 cd/m² to 52.7 cd/m². Copolymer IrCP-1 with the feed ratio of 1 mol% showed the highest L_{max} of 52.7 cd/m² at 11 V. However, copolymers IrCP-4 and IrCP-7 with the composition of 6.5 mol% and 33.3 mol% exhibited very poor emission.

Further increases in voltage over highest brightness cause attenuation in brightness for devices based on copolymers IrCP-1, IrCP-2, IrCP-3, CrCP-5 and IrCP-6. Figure 5(c) show the efficiency-luminance density characteristics. Copolymer IrCP-1 showed the highest current efficiency of 0.0257 cd/A. Like other electrophosphorescent materials, the current efficiency decay with higher iridium load possibly due to the triplet-triplet annihilation (TTA) becoming stronger in high triplet concentration.²⁵

As shown in Figure 6, EL spectra of copolymers IrCP-1, IrCP-2 and IrCP-3 appear to exhibit no emission corresponding to the iridium moiety, but only emission corresponding to the F8BT unit at about 540 nm. On the other hand, for IrCP-4, IrCP-5, and IrCP-6, the distinct emission corresponding to the iridium moiety was observed at about 650 nm in addition to the 540 nm that decays with high iridium moiety load. Note that the emission for the iridium moiety was completely

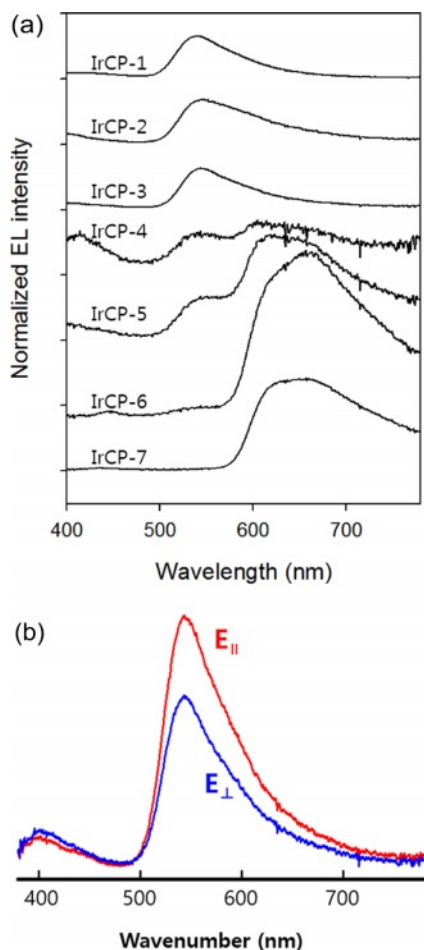


Figure 6. (a) EL spectra of copolymers; (b) EL spectra of IrCP-3 measured with the polarization parallel (\parallel) and perpendicular (\perp) to the rubbing direction.

quenched with 37.5 mol% feed ratio, *i.e.*, 33.3 mol% copolymer composition, probably due to the TTA with high triplet concentration.

In order to investigate the dichroism due to polarized light emission from the phosphorescent mesogenic polyfluorene, an iridium complex structure was introduced into benzothiadiazole copolymer chain, and the EML layer was planarly aligned by rubbing process. As shown in Figure 6(b), among all copolymers, IrCP-3 with the iridium-monomer content of 6.7 mol% in the copolymer composition showed the second highest L_{\max} of 35.6 cd/m² and J of 331 mA/cm². More noteworthy is that the IrCP-3 copolymer showed the most prominent dichroic ratio with a value of 1.47 among all the polymers.

Conclusions

In this study, a series of copolymers have been synthesized by the Suzuki coupling reaction with varying the feed ratio of dibromo-benzothiadiazole, dibromo-dioctylfluorene dibromide, and dibromo-phenylfluorene with a (piq)₂Ir(pic) side group. And their electroluminescence and dichroic properties were evaluated. First, the structure and composition of copolymers was investigated by FTIR and ¹H NMR spectroscopy. The results suggested that the composition of copolymers was somewhat different from the feed ratio. The Mn values of the copolymers were determined by GPC to be in the range of 6600 to 73000. The T_g and T_d of copolymers were 103 °C to 150 °C and 290 °C to 421 °C, respectively. In general, with increasing iridium content the T_g values tend to increase while T_d values to decrease. All copolymers showed broad diffraction patterns in the wide-angle region, and except for IrCP-4 and IrCP-5, the remaining copolymers showed a strong diffraction at small-angle region. UV-vis absorption spectra partially overlap with emission spectra, which indicates that the efficient energy transfer might be possible in this system. According to CV results, the bandgaps decreased with increasing iridium load.

Regarding electroluminescence, the high iridium load caused attenuation in current efficiency probably due to strong TTA. Among all copolymers, EL device of IrCP-1 with the iridium-monomer content of 1 mol% in the feed ratio shows the highest brightness, current density and efficiency. This might be attributed to efficient intramolecular energy transfer from the host to the guest. The important point to note is that a satisfactory dichroic ratio of 1.47 was achieved on the device based on IrCP-3 with the iridium-monomer content of 6.7 mol% in the copolymer composition.

Acknowledgments: This research was supported by Kumoh National Institute of Technology (2022-2023).

Conflict of Interest: The authors declare that there is no conflict of interest.

References

1. Sekine, C.; Tsubata, Y.; Yamada, T.; Kitano, M.; Doi, S. Recent Progress of High Performance Polymer OLED and OPV Materials for Organic Printed Electronics. *Sci. Technol. Adv. Mater.* **2014**, *15*, 034203.
2. Hack, M.; Weaver, M. S.; Brown, J. J. Status and Opportunities for Phosphorescent OLED Lighting. *SID Symposium Digest of Technical Papers*, **2017**, *48*, 187-190.
3. Fleischmann, E.; Zentel, R. Liquid-Crystalline Ordering as a Concept in Materials Science: From Semiconductors to Stimuli-Responsive Devices. *Angew. Chem. Int. Ed.*, **2013**, *52*, 8810-8827.
4. Wang, Y.; Shi, J.; Chen, J.; Zhu, W.; Baranoff, E. Recent Progress in Luminescent Liquid Crystal Materials: Design, Properties and Application for Linearly Polarised Emission. *J. Mater. Chem. C*, **2015**, *3*, 7993-8005.
5. O'Neill, M.; Kelly, S. M. Ordered Materials for Organic Electronics and Photonics. *Adv. Mater.* **2011**, *23*, 566-584.
6. Kitney, S. P. *Liquid Crystalline Semiconductors for Organic Electronics*; University of Hull: Hull, 2008.
7. Hu, G.; Billa, M. R.; Kitney, S. P.; Kitney, S. P. Symmetrical Carbazole-fluorene-carbazole Nematic Liquid Crystals as Electroluminescent Organic Semiconductors. *Liq. Cryst.* **2018**, *45*, 965-979.
8. Zou, G.; Luo, K. J.; Zhao, L.; Ni, H.; Wang, H.; Li, Q. Ortho-platinated Metallomesogens Based on Rod Mesogenic Unit of 2-Phenylpyridine Derivatives: Synthesis, High Linearly Polarized and Phase-state-dependent Luminescence. *Liq. Cryst.* **2018**, *45*, 593-606.
9. Aguiar, L. D.; Regis, E.; Tuzimoto, P.; Giroto, E.; Bechtold, I. H.; Gallardo, H.; Vieira, A. A. Investigation of Thermal and Luminescent Properties in 4,7-Diphenylethynyl-2,1,3-benzothiadiazole Systems. *Liq. Cryst.*, **2018**, *45*, 49-58.
10. Olate, F. A.; Parra, M. L.; Vergara, J. M.; Barberá, J.; Dahrouch, M. Star-shaped Molecules as Functional Materials Based on 1,3,5-Benzenetriesters with Pendant 1,3,4-Thiadiazole Groups: Liquid Crystals, Optical, Solvatochromic and Electrochemical Properties. *Liq. Cryst.*, **2017**, *44*, 1173-1184.
11. Kim, S.-W.; Lee, D.-M.; Kim, J.-H.; Choi, E.-J.; Yu, C.-J. Highly Polarised Electroluminescence in Low Aspect Ratio Mesogenic Molecules. *Liq. Cryst.* **2019**, *46*, 1136-1144.
12. Wang, Y.; Shi, J.; Chen, J.; Zhu, W.; Baranoff, E. Recent Progress in Luminescent Liquid Crystal Materials: Design, Properties and Application for Linearly Polarized Emission. *J. Mater. Chem. C*, **2015**, *3*, 7993-8005.
13. Grell, M.; Knoll, W.; Lupo, D.; Meisel, A.; Miteva, T.; Neher, D.; Nothofer, H.; Scherf, U.; Yasuda, A. Blue Polarized Electroluminescence from a Liquid Crystalline Polyfluorene. *Adv. Mater.* **1999**, *11*, 671-675.
14. Jo, S. I.; Kim, Y.; Baek, J. H.; Yu, C.-J.; Kim, J.-H. Highly Polarized Emission of the Liquid Crystalline Conjugated Polymer by Controlling the Surface Anchoring Energy. *Jpn. J. Appl. Phys.* **2014**, *53*, 03CD04.
15. Hou, Q.; Xu, Y.; Yang, W.; Yuan, M.; Peng, J.; Cao, Y. Novel Red-emitting Fluorene-based Copolymers. *J. Mater. Chem.* **2002**, *12*, 2887-2892.
16. Yersin, H. *Highly Efficient OLEDs with Phosphorescent Materials*; Wiley: Weinheim, 2008.
17. Knyazev, A.; Molostova, E. Y.; Krupin, A. S.; Heinrich, B.; Donnio, B.; Haase, W.; Galyametdinov, Y. Mesomorphic Behaviour and Luminescent Properties of Mesogenic Diketonate Lanthanide Adducts with 5,5'-Di(heptadecyl)-2,2'-bipyridine. *Liq. Cryst.* **2013**, *40*, 857-863.
18. Santoro, A.; Prokhorov, A. M.; Kozhevnikov, V. N.; Whitwood, A. C.; Donnio, B.; Williams, J. G.; Bruce, D. W. Emissive Metallomesogens Based on 2-Phenylpyridine Complexes of Iridium (III). *J. Am. Chem. Soc.* **2011**, *133*, 5248-5251.
19. Wong, M. Y.; Xie, G.; Tourbillon, C.; Sandroni, M.; Cordes, D. B.; Slawin, A. M.; Zysman-Colman, E. Formylated Chloro-bridged Iridium (III) Dimers as OLED Materials: Opening up New Possibilities. *Dalton Trans.*, **2015**, *44*, 8419-8432.
20. Singh, G.; Fisch, M. R.; Kumar, S. Tunable Polarized Fluorescence of Quantum Dot Doped Nematic Liquid Crystals. *Liq. Cryst.* **2017**, *44*, 444-452.
21. Liu, S.-H.; Lin, M.-S.; Chen, L.-Y.; Hong, Y.-H.; Tsai, C.-H.; Wu, C.-C.; Poloek, A.; Chi, Y.; Chen, C.-A.; Chen, S. H.; Hsu, H.-F. Polarized Phosphorescent Organic Light-emitting Devices Adopting Mesogenic Host-guest Systems. *Org. Electron.* **2011**, *12*, 15-21.
22. Honma, M.; Horiuchi, T.; Nose, T. Oblique Extraction of Polarized Light from Light-emitting Liquid Crystal Cells Doped with a Fluorescent Dye. *Jpn. J. Appl. Phys.* **2013**, *52*, 070205.
23. Chan, J. Y.; Lee, D.-M.; Han, J.-K.; Lee, Y.; Kim, S.-W.; Choi, E.-J.; Kim, J.-H. Circularly Polarized Emission from Mixture of Vacuum-Evaporated Mesogenic Luminophores. *Adv. Optical Mater.* **2022**, *10*, 2101674.
24. Wu, F. I.; Yang, X. H.; Neher, D.; Dodda, R.; Tseng, Y. H.; Shu, C. F. Efficient White-Electrophosphorescent Devices Based on a Single Polyfluorene Copolymer. *Adv. Funct. Mater.* **2007**, *17*, 1085-1902.
25. Adachi, C.; Baldo, M. A.; Forrest, S. R.; Thompson, M. E. High-efficiency Organic Electrophosphorescent Devices with Tris (2-phenylpyridine)iridium Doped into Electron-transporting Materials. *Appl. Phys. Lett.* **2000**, *77*, 904-906.

Publisher's Note The Polymer Society of Korea remains neutral with regard to jurisdictional claims in published articles and institutional affiliations.